World Neurosurgery: X 22 (2024) 100281

Contents lists available at ScienceDirect

World Neurosurgery: X

journal homepage: www.journals.elsevier.com/world-neurosurgery-x

One-step orbit reconstruction using PMMA implants following hyperostotic sphenoid wing meningioma removal: Evolution of the technique in short clinical series

Vadim S. Gadzhiagaev [a,*], Nikolay V. Lasunin [b], Dmitriy N. Okishev [a], Anton N. Konovalov [a], Denis A. Golbin [b], Vasily A. Cherekaev [b], Natalia K. Serova [c], Nadezhda N. Grigorieva [c]

[a] Burdenko Neurosurgical Center, Department of Cerebrovascular Surgery, 4th Tverskaya-Yamskaya Str. 16, Postal Index, Moscow, 125047, Russian Federation
[b] Burdenko Neurosurgical Center, Department of Cranio-Facial Surgery, 4th Tverskaya-Yamskaya Str. 16, Postal Index, Moscow, 125047, Russian Federation
[c] Burdenko Neurosurgical Center, Department of Neuro-ophthalmology, 4th Tverskaya-Yamskaya Str. 16, Postal Index, Moscow, 125047, Russian Federation

ARTICLE INFO

Keywords:
Meningioma
Sphenoid wing
Hyperostosis
Orbit
Reconstruction
Skull base
Proptosis

ABSTRACT

Purpose: To report our experience with patient specific implants for one-step orbit reconstruction following hyperostotic SWM removal and to describe the evolution of the technique through three surgical cases. Methods: Three cases of one-step SWM removal and orbit reconstruction are described. All cases are given consecutively to describe the evolution of the technique. Hyperostotic bone resection was facilitated by electromagnetic navigation and cutting guides (templates). Based on a 3D model, silicone molds were made using CAD/CAM. Then PMMA implant was fabricated from these molds. The implant was adjusted and fixed to the cranium with titanium screws after tumor removal. Results: Following steps of the procedure changed over these series: hyperostotic bone resection, implant thickness control, implant overlay features, anatomic adjustments, implant fixation. The proptosis resolved in all cases. In one patient the progressive visual acuity deterioration was recognized during the follow-up. No oculomotor disturbances and no tumor regrowth were found at the follow-up.

Conclusion: CAD/CAM technologies enable creation of implants of any size and configuration, and thereby, to increase the extent of bony resection and lower the risk of tumor progression. The procedure is performed in one step which decreases the risk of postoperative morbidity.

1. Introduction

The term hyperostotic sphenoid wing meningioma (SWM) is used to describe tumors involving the greater and lesser wings of the sphenoid bone with a soft component located in the orbit and middle cranial fossa. SWMs represent approximately 18% of all intracranial meningiomas,[1] and hyperostotic SWMs constitute approximately 4–7% of all intracranial meningiomas.[2,3]

Hyperostotic SWM is commonly diagnosed at its late stage and is characterized by a large extent of invasion. An optimal strategy for these patients is gross total resection with preservation of the critical structures and subsequent stereotactic radiation of the residual tumor. Hyperostotic bone in most cases contains neoplastic cells and as such should be removed during surgery.[4]

Despite high survival rates and a long recurrence-free period, surgery can lead to a reduction in quality of life due to major bony defects and new visual and oculomotor disorders.[5] Numerous studies have been published considering this topic.[3,6–9] Currently, the main issue is to provide a one-stage reconstruction of major postoperative skull defects.

In this study, we report our experience with patient-specific implants for one-step orbit reconstruction following hyperostotic SWM removal, details of preoperative planning of bone resection, implant making, surgical nuances and analysis of treatment results. Three surgical cases are given consecutively to describe the evolution of the technique.

* Corresponding author.
E-mail addresses: vgadzhiagaev@yandex.ru, vgadjiagaev@nsi.ru, ankonovalov@nsi.ru (V.S. Gadzhiagaev), lasunin@gmail.com (N.V. Lasunin), dokishev@nsi.ru (D.N. Okishev), ankonovalov@nsi.ru (A.N. Konovalov), dgolbin@nsi.ru (D.A. Golbin), vcherekaev@nsi.ru (V.A. Cherekaev), nserova@nsi.ru (N.K. Serova), ngrigoreva@nsi.ru (N.N. Grigorieva).

https://doi.org/10.1016/j.wnsx.2024.100281
Received 30 August 2022; Accepted 20 February 2024
Available online 25 February 2024

2. Materials and methods

All patients were operated on in the Burdenko Neurosurgery Center by one surgeon (NVL) in a short period of time. Early CT scans of the head with thin slices (<1 mm) were performed in all patients to reveal any residual tumor and assess the position of the implant and eye bulb. Clinical, cosmetic, and radiological outcomes (MRI) were assessed 6 months after surgery. All specimens were evaluated histologically.

The extent of resection was classified according to the Simpson grading system.[10]

2.1. Preoperative planning of the extent of bone resection

Thin slice MRI and CT scans were performed in all cases preoperatively. Virtual hyperostosis resection was performed with manual segmentation in the "Inobitec" DICOM viewer program. In all cases, the ipsilateral greater sphenoid wing was removed. The extent of surgical resection for the orbital roof, middle cranial fossa floor, and temporal squama varied between patients. In cases of compressive optic neuropathy, the lateral and superior walls of the optic canal were removed. It should be noted that involvement of the paranasal sinuses was regarded as a restrictive factor.

2.2. Implant modeling and manufacturing

CAD/CAM was performed using Inobitec Pro DICOM viewer, Meshmixer, and Blender support programs. A plastic template was formed based on the previously designed 3D model of the bone defect, which corresponded to the external resection boundaries. The templates were the most helpful when they formed the internal contour with the main fixation points located in the zygomatic processes of the temporal and frontal bones and the curvatures of the frontal and temporal bones (Fig. 1). The templates were sterilized using low-temperature sterilization system Sterrad 100NX.

Based on a 3D model, silicone molds were made using CAD/CAM (Fig. 2). They were sterilized with autoclaves sterilizer. Then, PMMA implants were fabricated from these molds. To obtain optimal results, PMMA material impregnated with antimicrobial agents (gentamycin) was put in press form for a 10-min polymerization (at an early stage). This allowed us to fill the mold cavity with PMMA. The implant was adjusted and fixed to the cranium with titanium screws after tumor removal.

Fig. 1. Cutting guide (template).

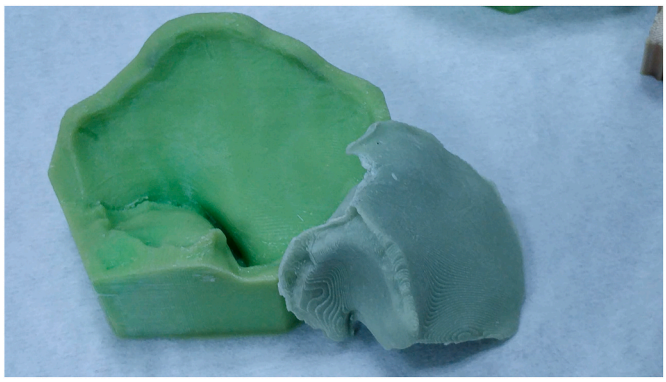

Fig. 2. Silicone molds and implant created intraoperatively.

2.3. Surgical technique

In all cases, an orbitozygomatic approach was performed. Electromagnetic navigation and plastic templates were used to reach the extent of resection planned preoperatively. Anterior clinoidectomy and optic canal deroofing were performed in 2 patients who had signs of compressive optic neuropathy. The templates facilitated fast hyperostosis resection of the calvarial part of the tumor. Its main fixation point was the frontal process of the zygoma. More fixation points were created to stabilize its position in patient 3. However, it required additional dissection of the temporal muscle down to the zygomatic arch. Neuronavigation was most helpful when drilling the middle cranial fossa floor and orbital roof during optic canal decompression and identification of the cavernous sinus, superior orbital fissure, and middle fossa foramina. In addition, the preplanned extent of the bone resection was uploaded into the electromagnetic frameless navigation system. It facilitated bone work significantly by allowing precise identification of predefined resection margins.

Intradural meningioma located around the sphenoid ridge was removed after hyperostosis resection. In two cases, intraorbital tumor extension was observed. This part of the tumor and infiltrated periorbita were resected as well. Sites of cavernous sinus and superior orbital fissure invaded by the tumor were coagulated.

2.4. Orbit reconstruction

An implant was placed via an arcuate trajectory. It was critically important to avoid any compression of the orbit between the implant and bone edges when installing an implant. It was achieved by an additional 1–2 mm overlay of an implant at the orbital roof site. Positioning of an implant at the orbital roof was performed under visual control, and then the outer edges of the implant and bone resection margins were fit together. If an implant seemed to be installed incorrectly in deep-seated regions, it was additionally checked by the navigation system. The superior orbital fissure part of the implant was formed with a 4–5 mm enlargement. A narrower fissure in the implant did not permit its linear installation. The inferior orbital fissure, anterior clinoid process, and middle cranial fossa floor were not reconstructed due to their insignificance and additional complexity.

Implant correction by a high-speed drill was required in cases of incorrect preoperative planning of bone resection and complexity caused by nonlinear implant positioning. All walls of the implant were minimized in thickness to provide a larger intracranial space. The PMMA implant was amenable for fast correction and precise placement. It should be noted that it would be impossible to install analogous titanium implants. Most often, it was necessary to make the following corrections: expansion of the superior orbital fissure, removal of the implant irregularities at the lesser sphenoid wing and the anterior clinoid process, reduction of the overlay size in the orbital roof region, and

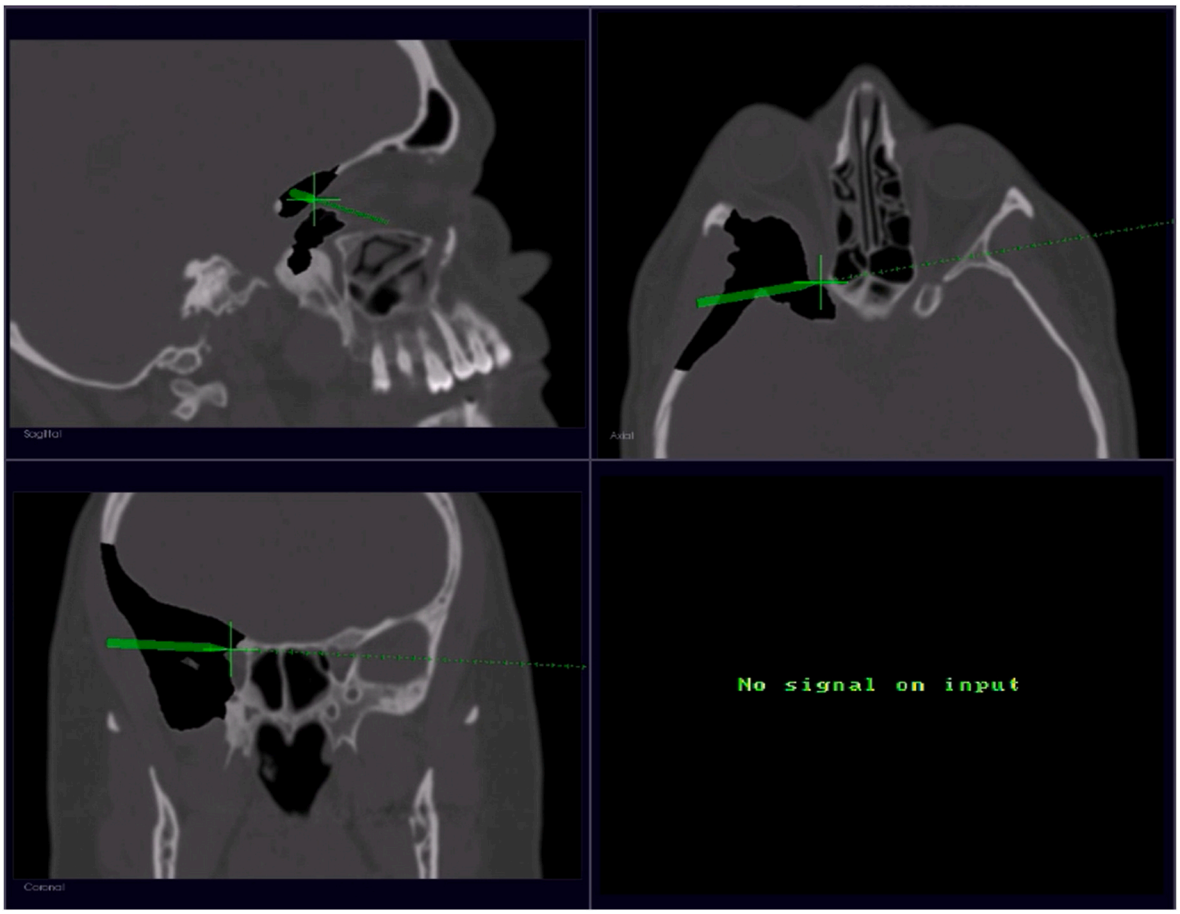

Fig. 3. Picture of the navigation system with uploaded DICOM series containing planned extent of resection.

removal of small irregularities from the anterolateral portions of the middle cranial fossa. The implant was then fixed with titanium screws. The position of the titanium screws was marked before the operation during the 3D-modeling process. In addition, the superior temporal line was modeled on an implant to determine the temporal muscle attachment. The orbito-zygomatic flap was placed and fixed, and soft tissues were sutured in a standard fashion.

3. Results

Baseline clinical and radiological data are shown in Tables 1 and 2. Two patients had decreased visual acuity after the operation. Both had undergone optic canal decompression. In one patient, visual deterioration was transient, and she had full recovery at the 6-month follow-up. In another patient, visual dysfunction was permanent and progressive: at the follow-up, she lost her vision in the left eye. Eye movement disturbances were noted in two patients. They were transient in all cases and resolved over time. One patient had persistent hyperpathic trigeminal pain in the V1 and V2 distribution. It required prolonged gabapentin administration. There was no evidence of other neurological complications or infection.

Complete removal of hyperostotic bone was achieved in all cases, which was demonstrated by the postoperative CT scan.

At the 6-month follow-up, there was complete resolution of exophthalmos in both patients who had it preoperatively. One of them had mild 2 mm proptosis in the early period after the operation because of orbital edema.

WHO grade I meningioma was confirmed in all cases. In 2 patients, tumor invasion of the bone was confirmed. None of the patients underwent postoperative radiotherapy due to the benign nature of the disease. On a follow-up MRI, there were no signs of tumor relapse.

Table 1
Pre-operative radiologic data, proptosis measurements pre-op, post-op and at follow-up.

№	Extent of hyperostosis	Pre-op proptosis, mm	Extent of resection[a]	Post-op proptosis, mm	FU proptosis, mm
1	The greater and lesser sphenoid wings (Fig. 3)	0	Grade II	0	0
2	The greater and lesser sphenoid wings, posterior part of the orbit and temporal squama, ACP	3	Grade II	0	0
3	The greater and lesser sphenoid wings, posterior orbital roof, and anterior part of the MCF, temporal squama, frontal bone, ACP	9 mm	Grade I	2	0

[a] According to the Simpson grading system, FU – follow-up, ACP – anterior clinoid process, MCF – middle cranial fossa.

3.1. Hyperostotic bone resection

In the last 2 patients, plastic templates were used for navigation of bone resection. As mentioned, the most efficient fixation point for the

Table 2
Pre-op, post-op, and follow-up ophthalmologic data.

№	Pre-op visual acuity	Post-op visual acuity	FU visual acuity	Post-op oculomotor dysfunction
1	1.00	1.00	1.00	–
2	0.80	0.20	0.00	Mild paresis out- and downward[a]
3	0.90	0.30	0.80	Mild paresis up- and inward[a]

[a] Transient, resolved over time.

template is the posterior margin of the zygomatic process of the frontal bone. However, the durability of such fixation was still not sufficient in case 2. Thus, in the third patient, an additional fixation point to the zygomatic arch was created. Template enabled fast determination of superficial bone resection margins and saved operative time. Nevertheless, electromagnetic navigation was indispensable for the removal of deeper hyperostotic zones. DICOM series containing the extent of the planned resection was uploaded into the navigation system in the last patient (Fig. 4). It allowed us to quickly reach the planned extent of resection of the orbital roof and prevented intraoperative correction of the corresponding part of the implant.

3.2. Thickness of implant

Implant thickness was minimized whenever possible to increase the intracranial space. It did not exhibit 4–5 at the convexity part. However, in the first patient, the thickness of the implant was greater than it was modeled. This was caused by the lack of exit pathways for PMMA release from the space between the molds. The number of these additional pathways was increased consecutively in both subsequent cases, and we did not face such problems in the third patient at all.

3.3. Implant overlay features

An implant overlay was created along the convex part (5–7 mm in width) as well as along the orbital part behind the lateral orbital rim (3–4 mm). The orbital part of the overlay was excessive in the first patient, and thus, implant placement was complicated. Additionally, the overlay size was too large in the convexity part in the second patient. Additional dissection of the temporal muscle was needed, and the cuff prepared earlier could not be used for muscle suturing in the second patient (Fig. 5). In the third patient, the convexity overlay was modified: it was created only at the fixation points (Figs. 6 and 7).

An additional 1–2 mm overlay was formed for the orbital roof. It allowed us to ensure a more secure position of an implant in the operative field and to avoid an implant shift toward the orbit as well as orbit compression in the adjacent area between the residual orbital roof margin and an implant. In addition, we found it very important to calculate the necessary length of titanium screws based on the thickness of the implant and the orbital wall.

3.4. Anatomic adjustments

The superior orbital fissure of the orbital part of the implant was too close in the first patient, and intraoperative high-speed drill correction was necessary. Subsequently, in two other cases, the superior orbital fissure in the implant was formed with a 4–5 mm enlargement. A narrower fissure in the implant does not permit its linear placement.

In the last case, the artificial superior temporal line was also marked on the implant for subsequent temporal muscle suturing (Fig. 7).

3.5. Implant fixation

Four fixation points along the convex part of the implant are usually sufficient. The implant is fixated with titanium screws. Fixation points were also marked during the modeling stage in the last two cases.

4. Discussion

Since its appearance, cranial reconstruction has undergone considerable changes: it has evolved from primitive split bone flaps to patient-

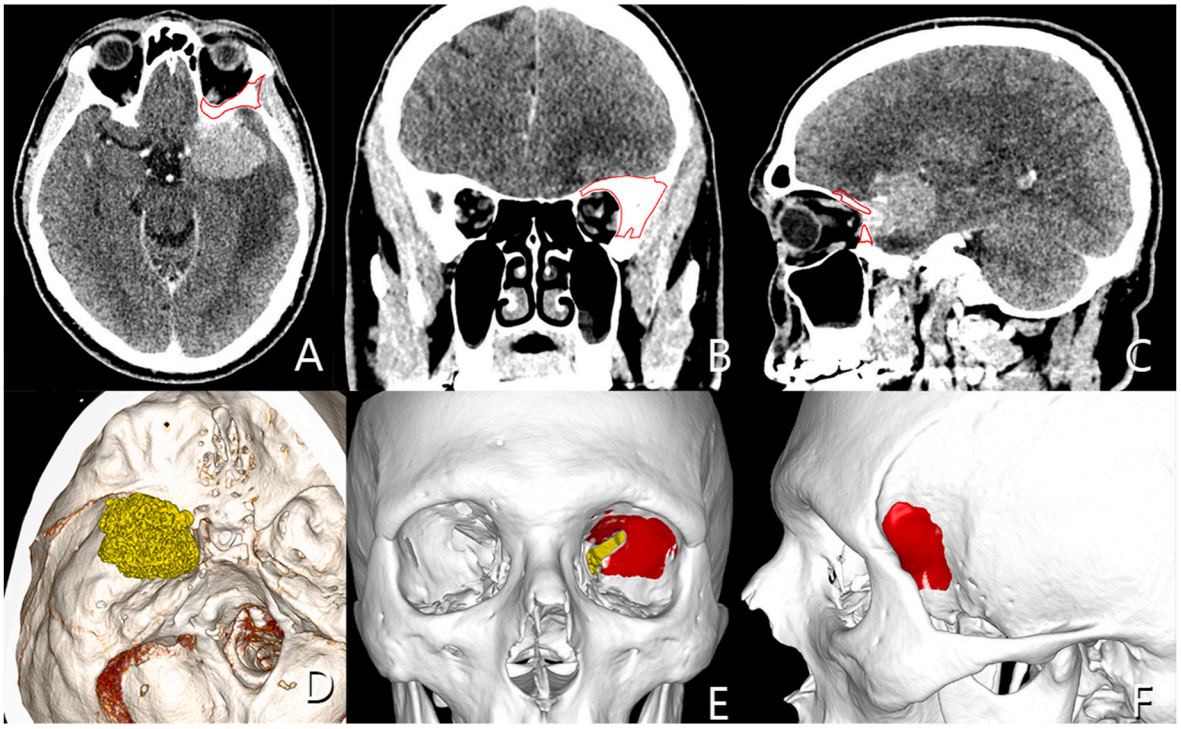

Fig. 4. Patient 1. (A–C) Pre-op CT scan, extent of hyperostosis. (D–F) 3D CT scan, intradural tumor soft component (yellow), extent of hyperostosis (red). (For interpretation of the references to colour in this figure legend, the reader is referred to the web version of this article.)

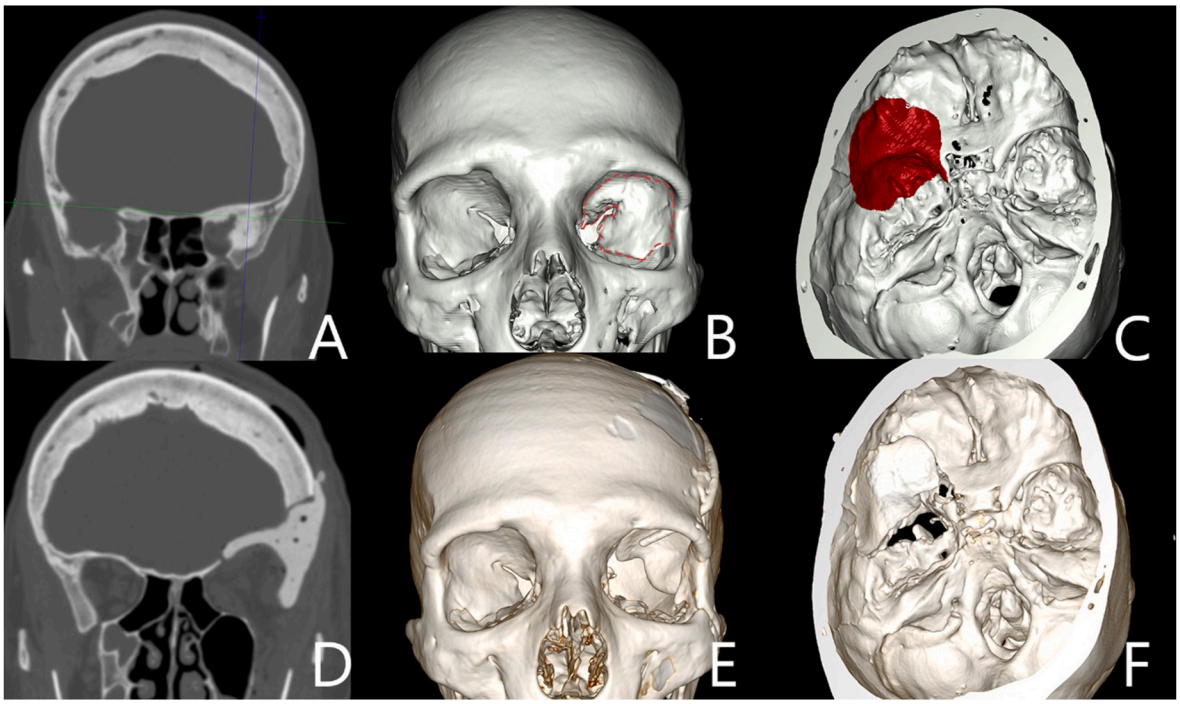

Fig. 5. Patient 2. (A–C) Pre-op CT scan showing extent of hyperostosis. (D–F) Post-op CT scan showing position if the implant.

specific implants. Today, we deal with the following set of problems: 1) search for the ideal material; 2) technological aspects - implant modeling and fabrication; and 3) surgical aspects - preoperative planning of the extent of resection, adequate tumor resection according to the preoperative plan, placement and fixation of complex implants.

The introduction of CAD/CAM into the surgical treatment of these patients allowed surgeons to significantly improve outcomes. There are a limited number of studies describing this technology, and reconstruction is usually reported as a separate surgical procedure performed a few months after tumor removal.

This technique enables surgeons to reconstruct the normal skull anatomy more completely and accurately and thus significantly improve functional and cosmetic results. The main drawback of this treatment modality is its staging. The inability to reconstruct bone defects during the first procedure for some surgical and technical reasons results in an increased risk of complications (CSF leakage, infections, development of meningocele, restrictive oculomotor disorders, pulsating enophthalmos), long hospital stay and treatment course, recurrent hospitalization, and repeated trauma to soft tissues.

The high-quality CAD/CAM potentiates simultaneous tumor resection and skull defect reconstruction by a patient-specific 3D-printed implant. At the moment, this technique raises a number of unanswered questions due to its rare use in routine practice, lack of detailed technical and surgical guides, and descriptions of series of cases with outcome analysis.

4.1. Literature analysis

We reviewed 14 studies dedicated to surgery for hyperostotic SWMs published since 2011 (Table 3). In some studies, no reconstruction of the orbit was performed.[3,6–9] The following materials were used in the remaining studies: titanium mesh,[5,11–14] porous polyethylene,[15,16] and split grafts.[17,18]

A selective approach in terms of rigid orbit reconstruction is most common. It is considered to be required in cases of extensive lateral orbital wall and orbital roof removal during surgery. In addition, the risk of enophthalmos increases with resection of the periorbita. In such cases, when appropriate reconstruction is not performed, the risk approaches 5% according to the literature. However, some authors report reasonable cosmetic results without any rigid reconstruction.[9] At the same time, Terrier et al reported 130 patients.[5] In most patients, orbit reconstruction was performed. These patients achieved significantly better cosmetic outcomes. In particular, temporal muscle atrophy was less frequently encountered in this group.

The rate of proptosis resolution was very high in most studies (up to 100%). It was less than 70% in only 2 studies.[5,9] However, Terrier et al reported on the treatment of 130 patients, and this is the largest series in the literature. Thus, the lower rate of proptosis resolution described by the authors (60%) might reflect the actual efficacy of surgical treatment of hyperostotic SWMs.

One case of pulsating exophthalmos was described in a series by Talacchi et al..[3] It was suggested to occur due to inappropriate frontal dural suspension. Postoperative enophthalmos developed in 3 patients in a series by Terrier et al; however, there is no information about the type of orbit reconstruction in these patients. In a series by Nagahama et al, 2 patients had enophthalmos postoperatively, and none of them underwent orbit reconstruction during the operation.[18]

4.2. Implant material

The main factors defining an optimal implant material for skull reconstruction are 1) small thickness (range 0,3–0,5 mm) of some of its walls and 2) possible correction (additional partial implant correction) during surgery.

Even when a serious dynamic load on the implant walls is absent during fixation, the static load can be formed in the thinnest segments of the implant. An implant material should have the appropriate toughness and hardness.

Earlier split bone grafts from different donor sites were used for cranial defect reconstruction: iliac crest[19] and inner table of skull bones. Later, alloplastic metallic materials (titanium mesh) and nonmetallic (polymer) materials were implemented, such as PMMA, polyether-ether-ketone (PEEK), glass-ceramic, porous polyethylene, polylactide, and different types of calcium hydroxyapatite.

Among autologous implants, the most popular are split bone grafts. Their use is limited to small defects. If used for large-size defects, a

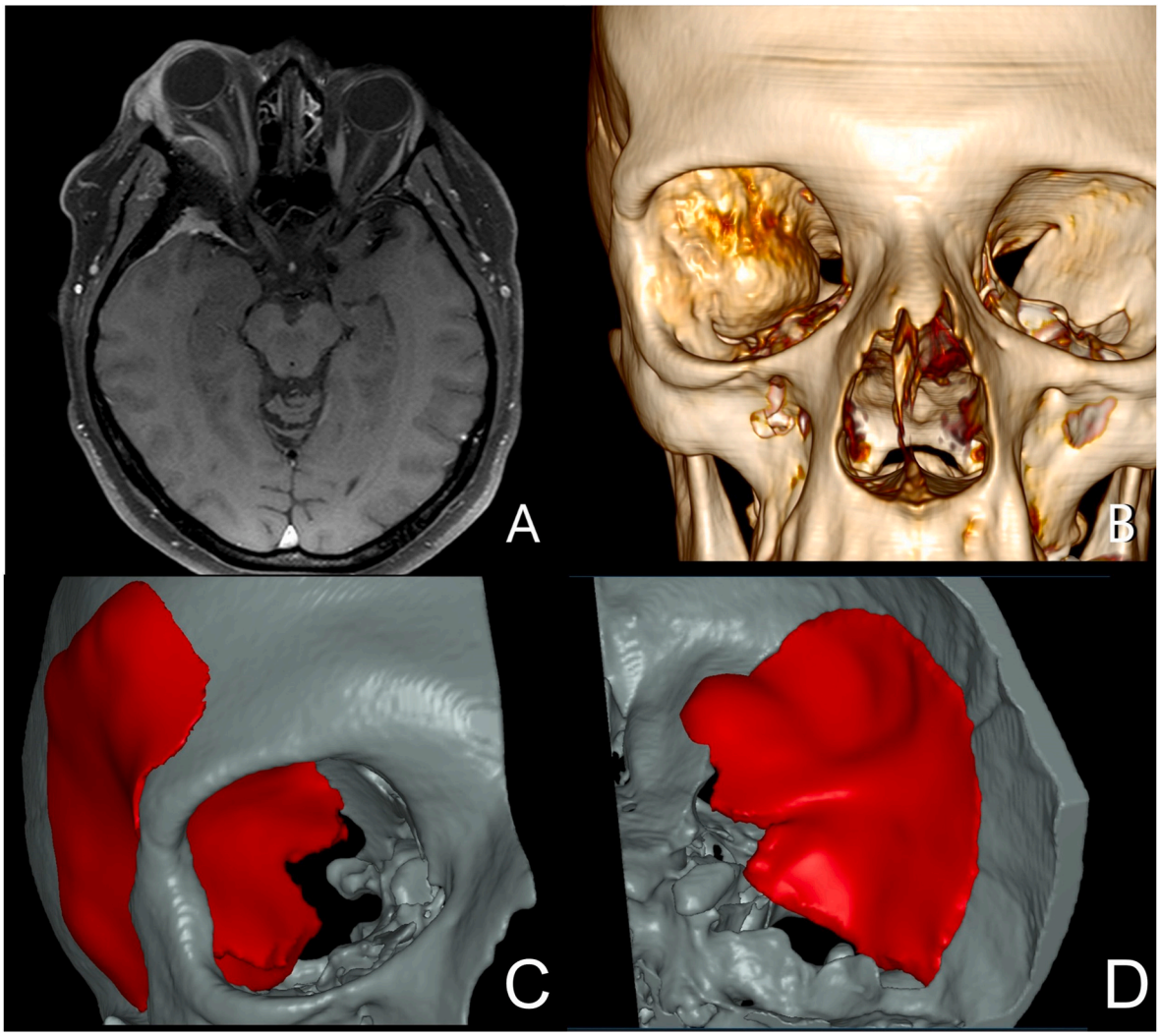

Fig. 6. Patient 3. (A) Pre-op MRI showing hyperostotic area, intradural and intraorbital tumor components. (B) Pre-op 3D CT scan, frontal view, hyperostotic bone growing into the orbit is easily recognizable. (C, D) Post-op CT scan showing the position of the implant.

neurosurgeon may face difficulties with implant shaping and fixation due to the increased risk of donor-site complications as well as cosmetic and functional problems caused by bone resorption in the follow-up period. Autografts from the iliac crest and rib are also less favored for similar reasons.

Hattori et al.[20] described preoperative planning of cranial bone reconstruction using a stereolithographic model in 3 patients with hyperostotic cranio-orbital meningiomas. Tumor removal was followed by simultaneous skull defect reconstruction by a patient-specific titanium mesh. Our experience shows that a variety of unpredicted nuances at the initial stage of introducing new technology into clinical practice required regular implant shape correction during operation. The use of titanium mesh makes this correction impossible, thus forcing a surgeon to perform risky manipulations for extra skull bone resection or even to exclude implant installment.

Currently, PMMA is widely used in cranial vault reconstruction.[21,22] The material is known to have satisfactory neuroimaging characteristics and is tolerant to radiosurgical treatment. Ringel et al and Scarone et al reported on PMMA implant application for cranioorbital reconstruction.[23,24]

PMMA is similar to bone tissue by its mechanical characteristics; it can be easily corrected intraoperatively. In addition, there is no risk of thermal damage to the adjacent tissues due to polymerization because an implant is formed using molds.

At the same time, Matsuno et al and Lee et al reported on cases of infection and implant rejection.[22,25] These risks are significantly increased when nasal sinuses are injured during surgical intervention and an implant comes into contact with sinuses, even when isolated by autologous tissues. For these reasons, we used PMMA impregnated with antimicrobial agents (gentamycin).

An additional limiting factor is implant complexity. Fabrication of PMMA implants for orbital reconstruction is extremely difficult due to their complicated extraction from the mold after polymerization. Today, silicone molds have proven to be highly effective, considerably simplifying the process of implant formation.

PEEK is another polymer material that is popular in skull defect reconstruction. Its application was described in a large number of publications,[26,27] where PEEK was demonstrated to have satisfactory mechanical properties, was compatible with modern imaging technologies, was tolerant to radiotherapy, and was easy to handle. The main disadvantage of PEEK is the high fragility of thin walls. According to Jonkergouw et al, the incidence of infectious complications was 13% in a series of 40 patients, and an implant was removed in each of these cases.[27]

4.3. *Implant fabrication*

The spheno-orbital region could be geometrically described as a

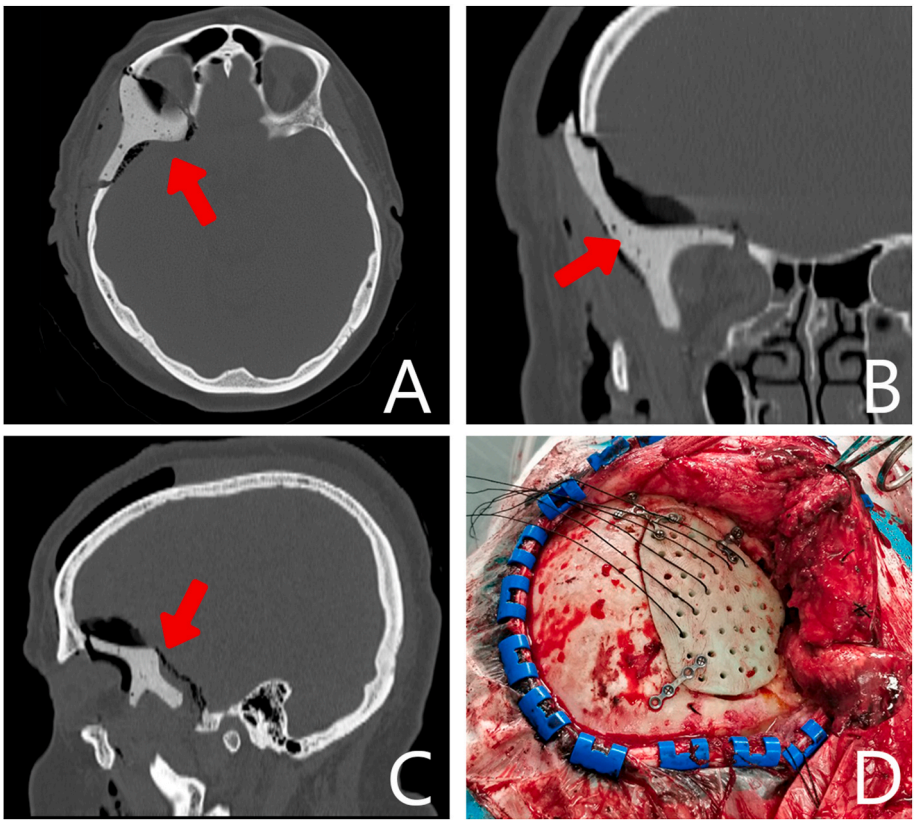

Fig. 7. Patient 3. (A–C) Post-op CT scan. (D) Intraoperative picture.

Table 3
Literature review.

Authors, publication year	Sample size	Material of reconstruction	Proptosis resolution, %	Neurologic complications	Implant-related infection
Oya et al, 2011[39]	39	No reconstruction	73,5%	Visual dysfunction, facial hypoesthesia, decreased eye movements	0
Chambless et al, 2012[40]	12	Porous polyethylene	91,7%	–	1[a]
Marcus et al, 2013[38]	19	Titanium mesh	100%	Visual dysfunction, ptosis, facial hypoesthesia	0
Boari et al, 2013[12]	40	Titanium mesh	92,5%	Visual dysfunction, decreased eye movements	2[b]
Talacchi et al, 2014[3]	47	No reconstruction	91.1%	Visual dysfunction, decreased eye movements, chronic neuropathic pain	1[b]
Çıkarılmasında et al, 2014[16]	13	Porous polyethylene	80%	–	0
Leroy et al, 2016[17]	70	Split bone flaps	86%	Visual dysfunction, decreased eye movements	0
Bowers et al, 2016[7]	33	No reconstruction	78,8%	Visual dysfunction, facial hypoesthesia	0
Peron et al, 2017[8]	30	No reconstruction	100%	Visual dysfunction, abducens nerve deficiency	0
Gonen et al, 2017[13]	27	Titanium mesh	77%	Visual dysfunction	0
Freeman et al, 2017[14]	25	Titanium mesh	86,3%	Cerebral ischemia and edema	1[b]
Terrier et al, 2018[5]	130	Titanium mesh -58, PMMA – 18, split bone flaps – 4	60%	Visual dysfunction, facial hypoesthesia, decreased eye movements, cerebral ischemia, cerebral venous thrombosis	2
Nagahama et al, 2019[18]	12	Split bone flaps	70%	Visual dysfunction, facial hypoesthesia, decreased eye movements, cerebral ischemia	0
Menon et al, 2020[9]	17	No reconstruction	64,3%	Visual dysfunction, decreased eye movements, chronic neuropathic pain	0

PMMA – polymethyl-methacrylate.
[a] Did not require implant removal.
[b] Required implant removal.

frustum with the additional planes fixed to its external surface. The thickness of the bone walls varied widely from 0,3–10 mm. The methods of fabricating patient-specific implants depend on the reconstruction material.

"Handmade" implant making does not require any special skills and knowledge in 3D modeling from an operating surgeon, but its level of precision is much lower. The most frequently used models (variants) of this technology are titanium mesh and titanium-based multicomponent autologous bone constructions.

Titanium mesh is another material that is commonly used for simultaneous cranio-orbital reconstruction, with the assistance of hand-made design technologies. It allows satisfactory results to be achieved for small-sized and simple-shaped cranial defects. However, it does not ensure an adequate mechanical resistance of reconstruction when

dealing with large-sized cranial defects. In addition, it lacks precision.

Westendorff et al tried to address these challenges[28] by producing a multipiece implant consisting of a titanium core and titanium mesh. The shape of the implant was amenable to adjustments during surgery to match the cranial defect.

CAD/CAM of molds provides simpler conditions for sterilization of implant material. It is less expensive and takes less time (10–15 min) if the first implant has been damaged, and a new implant is needed. One of the disadvantages of this technique is the increase in surgical time due to the partial implant making in the operating room. 3D-printing technology provides a final product, thus reducing the operating time. However, damage or poor sterility of an implant may be risky for the entire process of reconstruction. In addition, there are strict requirements for the methods and quality of sterilization, storage and transportation of the product.

4.4. Extent of bone resection and cranial defect reconstruction

Preoperative planning of the extent of resection is extremely important for effective one-stage cranioorbital reconstruction.

Before installing the PMMA implant in 2 patients with hyperostotic SWM, Pritz et al planned the extent of bone resection using a stereolithographic model.[29] No technologies were used to compare the intraoperative extent of bone resection with that performed on a stereolithographic model. Della Puppa et al applied a similar technique for planning the extent of resection of convexital osteoma with further reconstruction by an implant made of hydroxyapatite.[30] It is evident that under these conditions, it is hardly possible to achieve the planned extent.

Gerbino et al described the technique of using special templates for specifying the resection boundaries.[31] As soon as a patient-specific implant was modeled, a patient-specific cutting guide was planned and produced. To perform reconstruction immediately after removal of craniofacial fibrous dysplasia in 2 patients, Eppley et al planned bone resection on stereolithographic models. He also used silicone templates for the intraoperative navigation of bone resection.[32] This complicated technique was also described by Vougioukas et al and Eufinger et al..[33–35] The key drawback of this method is its unusefulness in assessing the depth of bone resection, particularly in the orbital roof, superior and inferior orbital fissure, optic canal, and middle cranial fossa.

Rosen et al planned resection of extensive fibrous dysplasia based on a stereolithographic model. Moreover, intraoperatively, he used a template and frameless navigation. This method is more progressive and helpful in controlling the extent of bone resection in the depth of the operative field. One of the disadvantages of this technique is the prolonged operative time.

In our opinion, an optimal algorithm is the combination of a prototyping template and intraoperative navigation with preoperative uploading of the planned resection extent into the navigation system. This technique was also reported by Jalbert et al; it provides maximally fast and accurate control of the extent of hyperostotic resection.[36]

Intraoperative difficulties with prefabricated implants are described by Gerbino et al and Jalbert et al.[26,37] The novelty of this technology and lack of sufficient practical experience make each operation unique. There are no guidelines for determining the sequence and extent of resection regarding further high precision installment of an implant. There are also no algorithms for implant modeling depending on the extent of cranial reconstruction and specificities of the zones to be reconstructed. For the moment, this field of study is mostly unexplored; however, it is very actual.

4.5. Orbit volume

Another difficult problem is providing volume symmetry in orbital reconstruction to achieve optimal cosmetic and functional results, including the eyeball position. Menon et al calculated orbital volumes in a series of 17 patients. However, the authors did not perform rigid orbit reconstruction at all.[9] Our first experience and follow-up data showed that the final soft tissue volume of the operated orbit was less than that of the healthy orbit. Most likely, the main reason for this was partial atrophy of the orbital fat due to continuous compression by the tumor. Hence, similar orbital volumes may result in enophthalmos formation at the operative site. An additional analysis and prognosis of the adequate (but not similar) orbital volume is beyond the limitations of the present study. However, it could be important for the achievement of optimal outcomes and should be further investigated.

4.6. Postoperative complications

Hyperostotic SWM removal often leads to a variety of neurological complications. Visual deterioration, eye movement dysfunction, ptosis, and trigeminal hyper/hypoesthesia are most common.

The incidence of visual dysfunction postoperatively was 30–66.7% in the reviewed literature. In the study of Marcus et al, visual deterioration was revealed in 57,9% of patients, and 5,3% became blind.[38] Two patients in our series had decreased visual acuity after the operation. We performed optic canal decompression in both cases due to encasement of its roof and the anterior clinoid process by hyperostosis. Unfortunately, one patient appeared to lose vision in her left eye at the 6-month follow-up.

Trigeminal nerve dysfunction and eye movement disturbances are common but usually resolve over time. Different combinations of oculomotor, trochlear and abducens palsy are encountered in 10–13.3% of cases. Orbital edema is another reason that leads to transient limitations of eye movements, which was observed in two of our patients. Hyperpathic trigeminal pain usually requires a short period of gabapentin or carbamazepine. However, in one of our patients, it became permanent and progressive.

In addition to these minor complications, neurological catastrophes such as brain swelling, cerebral ischemia and cerebral venous thrombosis were described in the analyzed series.[5,14,18]

4.7. Postoperative radiotherapy

Postoperative radiotherapy was not considered in our patients due to total or subtotal resection of the tumors (Simpson grade I or II), benign nature of disease (WHO Grade I), and no signs of regrowth on a follow-up. In a series by Terrier et al, 2 patients underwent radiotherapy early after the operation due to residual tumor, and 10 patients underwent radiotherapy later due to regrowth.[5] It did not lead to decubitus at the wound site or implant rejection. Authors do not support aggressive strategy with radiotherapy and prefer to closely observe the patients rather than risk any further damage. Data concerning implant-related complications after radiotherapy are scarce in the literature. It is a subject of further investigation. The effect of radiation modalities on tumor growth and implant tolerance should be assessed by long-term follow-up series.

4.8. Limitations of the study

This study is limited by its retrospective design and small number of patients. Another limitation is the absence of patients after radiotherapy and scarce data on grade II/III sphenoid wing meningiomas.

Additional limitations imposed by a retrospective study design, such as different surgical strategies among patients and variability between observers in assessing the extent of resection, must be considered when interpreting the results. Nonetheless, our study focused more on surgical nuances of adequate one-step removal of sphenoid wing meningiomas and rigid orbit reconstruction.

5. Conclusion

The advantages of using cranial reconstruction and implant installment during one surgical procedure are evident. The possibility of building different implant shapes and sizes allows us to remove bone as far as possible up to the "tumor-free resection boundaries" and as such to decrease the danger of tumor regrowth and provide optimal functional and cosmetic results with one surgical procedure.

Cranial bone reconstruction by a patient-specific implant after removal of hyperostotic cranio-orbital meningioma is a technically difficult and tricky procedure, the success of which depends on the surgeon's experience. Preoperative planning using CAD is of vital importance and involves a team of professionals.

There is a further need for modifying the methods of preoperative planning and intraoperative navigation of bone resection, searching for "ideal" material for reconstruction and developing guidelines for surgical resection and implant placement in these patients.

Ethical approval

All procedures performed in studies involving human participants were in accordance with the ethical standards of the institutional research committee and with the 1964 Helsinki declaration and its later amendments or comparable ethical standards.

Funding

This research did not receive any specific grant from funding agencies in the public, commercial, or not-for-profit sectors.

Informed consent

Informed consent was obtained from all individual participants included in the study.

CRediT authorship contribution statement

Vadim S. Gadzhiagaev: Conceptualization, Methodology, Writing – original draft. **Nikolay V. Lasunin:** Methodology, Writing – original draft, Investigation, Conceptualization. **Dmitriy N. Okishev:** Resources, Visualization, Writing – review & editing, Methodology, Software. **Anton N. Konovalov:** Visualization, Software. **Denis A. Golbin:** Writing – review & editing, Supervision. **Vasily A. Cherekaev:** Writing – review & editing, Supervision. **Natalia K. Serova:** Methodology. **Nadezhda N. Grigorieva:** Methodology.

Declaration of competing interest

The authors declare that they have no known competing financial interests or personal relationships that could have appeared to influence the work reported in this paper.

Acknowledgment

This research did not receive any specific grant from funding agencies in the public, commercial, or not-for-profit sectors.

Abbreviations

CAD/CAM	computer-aided design and computer-aided manufacturing
CT	computerized tomography
FU	follow-up
IOF	inferior orbital fissure
MCF	middle cranial fossa
MRI	magnetic resonance imaging
PMMA	polymethyl-metacrylate
PEEK	polyether ether ketone
SOF	superior orbital fissure
SWM	sphenoid wing meningioma

References

1. Maroon JC, Kennerdell JS, Vidovich DV, Abla A, Sternau L. Recurrent spheno-orbital meningioma. *J Neurosurg*. 1994;80(2):202–208. https://doi.org/10.3171/jns.1994.80.2.0202.
2. De Jesus O, Toledo MM. Surgical management of meningioma en plaque of the sphenoid ridge. *Surg Neurol*. 2001;55(5):265–269.
3. Talacchi A, De Carlo A, D'Agostino A, Nocini P. Surgical management of ocular symptoms in spheno-orbital meningiomas. Is orbital reconstruction truly necessary? *Neurosurg Rev*. 2014;37(2). https://doi.org/10.1007/s10143-014-0517-y.
4. Alzhrani G, Couldwell W. Bony hyperostosis recurrence after complete resection of sphenoorbital meningioma. *Cureus*. 2017;9(8), e1540. https://doi.org/10.7759/cureus.1540.
5. Terrier L-M, Bernard F, Fournier H-D, et al. Spheno-orbital meningiomas surgery: multicenter management study for complex extensive tumors. *World Neurosurg*. 2018;112:e145–e156. https://doi.org/10.1016/j.wneu.2017.12.182.
6. Oya S, Lee JH. Sphenoorbital meningioma: surgical technique and outcome (vol 114, pg 1241, 2011). *J Neurosurg*. 2011;114(5):1485. https://doi.org/10.3171/2011.1.JNS101128a.
7. Bowers CA, Sorour M, Patel BC, Couldwell WT. Outcomes after surgical treatment of meningioma-associated proptosis. *J Neurosurg*. 2016;125(3):544–550. https://doi.org/10.3171/2015.9.JNS15761.
8. Peron S, Cividini A, Santi L, Galante N, Castelnuovo P, Locatelli D. Spheno-Orbital meningiomas: when the endoscopic approach is better. *Acta Neurochir Suppl*. 2017. https://doi.org/10.1007/978-3-319-39546-3_19.
9. Menon S, Sandesh O, Anand D, Menon G. Spheno-orbital meningiomas: optimizing visual outcome. *J Neurosci Rural Pract*. 2020;11(3):385–394. https://doi.org/10.1055/s-0040-1709270.
10. Simpson D. The recurrence of intracranial meningiomas after surgical treatment. *J Neurol Neurosurg Psychiatry*. 1957;20(1):22–39. https://doi.org/10.1136/jnnp.20.1.22.
11. Marcus J, Laufer I, Mehrara B, Kraus D, Singh B, Bilsky MH. Anterior and anterolateral resection for skull base malignancies: techniques and complication avoidance. *Neurosurg Clin*. 2013;24(1):11–18. https://doi.org/10.1016/j.nec.2012.08.008.
12. Boari N, Gagliardi F, Spina A, Bailo M, Franzin A, Mortini P. Management of spheno-orbital en plaque meningiomas: clinical outcome in a consecutive series of 40 patients. *Br J Neurosurg*. 2013;27(1):84–90. https://doi.org/10.3109/02688697.2012.709557.
13. Gonen L, Nov E, Shimony N, Shofty B, Margalit N. *Sphenoorbital Meningioma: Surgical Series and Design of an Intraoperative Management Algorithm*. 2017:1–11. https://doi.org/10.1007/s10143-017-0855-7.
14. Freeman JL, Davern MS, Oushy S, et al. Spheno-orbital meningiomas: a 16-year surgical experience. *World Neurosurg*. 2017;99:369–380. https://doi.org/10.1016/j.wneu.2016.12.063.
15. Chambless LB, Mawn LA, Forbes JA, Thompson RC. Porous polyethylene implant reconstruction of the orbit after resection of spheno-orbital meningiomas: a novel technique. *J Cranio-Maxillo-Fac Surg*. 2012;40(1):e28–e32. https://doi.org/10.1016/j.jcms.2011.01.016.
16. Çıkarılmasında SM, Stratejiler C, Solmaz I, et al. Surgical strategies for the removal of sphenoorbital meningiomas. *Orig Investig Turk Neurosurg*. 2014;24(6):859–866. https://doi.org/10.5137/1019-5149.JTn.10336-14.3.
17. Leroy H-A, Leroy-Ciocanea CI, Baroncini M, et al. Internal and external spheno-orbital meningioma varieties: different outcomes and prognoses. *Acta Neurochir*. 2016;158(8):1587–1596. https://doi.org/10.1007/s00701-016-2850-0.
18. Nagahama A, Goto T, Nagm A, et al. Sphenoorbital meningioma: surgical outcomes and management of recurrence. *World Neurosurg*. 2019:1–9. https://doi.org/10.1016/j.wneu.2019.02.123.
19. Columella F, Testa C, Andreoli A. Radical resection and reconstruction in spheno-ethmoidal-orbital tumors. Report of 3 cases. J Neurosurg Sci. 18(3):198-205. http://www.ncbi.nlm.nih.gov/pubmed/4377275. Accessed November 16, 2017..
20. Hattori N, Nakajima H, Tamada I, et al. Evaluation of three cases using a novel titanium mesh system-Skull-Fit® with orbital wall (Skull-Fit WOW®)-for cranial base reconstructions. *Skull Base*. 2011;21(5):279–286. https://doi.org/10.1055/s-0031-1280684.
21. Cophignon J, Lucena J, Clay C, Marchac D. Limits to radical treatment of spheno-orbital meningiomas. *Acta Neurochir Suppl*. 1979;28(2):375–380.
22. Matsuno A, Tanaka H, Iwamuro H, et al. Analyses of the factors influencing bone graft infection after delayed cranioplasty. *Acta Neurochir*. 2006;148(5):535–540. https://doi.org/10.1007/s00701-006-0740-6.
23. Ringel F, Cedzich C, Schramm J. Microsurgical technique and results of a series of 63 spheno-orbital meningiomas. *Neurosurgery*. 2007;60(4 Suppl 2):212–214. https://doi.org/10.1227/01.NEU.0000255415.47937.1A.
24. Scarone P, Leclerq D, Heran F, Robert G. Long-term results with exophthalmos in a surgical series of 30 sphenoorbital meningiomas. Clinical article. *J Neurosurg*. 2009;111(5):1069–1077. https://doi.org/10.3171/2009.1.JNS081263.
25. Lee SC, Wu CT, Lee ST, Chen PJ. Cranioplasty using polymethyl methacrylate prostheses. *J Clin Neurosci*. 2009;16(1):56–63. https://doi.org/10.1016/j.jocn.2008.04.001.

26. Brandicourt P, Delanoé F, Roux FE, Jalbert F, Brauge D, Lauwers F. Reconstruction of cranial vault defect with polyetheretherketone implants. *World Neurosurg.* 2017; 105:783–789. https://doi.org/10.1016/j.wneu.2017.04.049.
27. Jonkergouw J, van de Vijfeijken SECM, Nout E, et al. Outcome in patient-specific PEEK cranioplasty: a two-center cohort study of 40 implants. *J Cranio-Maxillofacial Surg.* 2016;44(9):1266–1272. https://doi.org/10.1016/j.jcms.2016.07.005.
28. Westendorff C. *Technical case reports image-guided sphenoid wing meningioma resection and simultaneous computer-assisted*, 60. 2007. https://doi.org/10.1227/01.NEU.0000249235.97612.52.
29. Pritz MB, Burgett RA. Spheno-orbital reconstruction after meningioma resection. *Skull Base.* 2009;19(2):163–170. https://doi.org/10.1055/s-0028-1096199.
30. Della Puppa A, Rustemi O, Gioffrè G, et al. Predictive value of intraoperative 5-aminolevulinic acid–induced fluorescence for detecting bone invasion in meningioma surgery. *J Neurosurg.* 2014;120(4):840–845. https://doi.org/10.3171/2013.12.JNS131642.
31. Gerbino G, Bianchi FA, Zavattero E, Tartara F, Garbossa D, Ducati A. Single-step resection and reconstruction using patient-specific implants in the treatment of benign cranio-orbital tumors. *J Oral Maxillofac Surg.* 2013;71(11):1969–1982. https://doi.org/10.1016/j.joms.2013.03.021.
32. Eppley BL, Kilgo M, Coleman JJ. Cranial reconstruction with computer-generated hard-tissue replacement patient-matched implants: indications, surgical technique, and long-term follow-up. *Plast Reconstr Surg.* 2002;109(3):864–871. https://doi.org/10.1097/00006534-200203000-00005.
33. Spetzger U, Vougioukas V, Schipper J. Materials and techniques for osseous skull reconstruction. *Minim Invasive Ther Allied Technol.* 2010;19(2):110–121. https://doi.org/10.3109/13645701003644087.
34. Vougioukas VI, Hubbe U, Van Velthoven V, Freiman TM, Schramm A, Spetzger U. Neuronavigation-assisted cranial reconstruction. *Neurosurgery*. 2004;55(1):162–167. https://doi.org/10.1227/01.NEU.0000126940.20441.E7.
35. Eufinger H, Wittkampf ARM, Wehmoller M, Zonneveld FW. Single-step fronto-orbital resection and reconstruction with individual resection template and corresponding titanium implant: a new method of computer-aided surgery. *J Cranio-Maxillofacial Surg.* 1998;26(6):373–378. https://doi.org/10.1016/S1010-5182(98)80070-X.
36. Jalbert F, Boetto S, Nadon F, et al. One-step primary reconstruction for complex craniofacial resection with PEEK custom-made implants. *J Cranio-Maxillofacial Surg.* 2014;42(2):141–148. https://doi.org/10.1016/j.jcms.2013.04.001.
37. Gerbino G, Zavattero E, Zenga F, Bianchi FA, Garzino-demo P, Berrone S. Primary and secondary reconstruction of complex craniofacial defects using polyetheretherketone custom-made implants. *J Cranio-Maxillofacial Surg.* 2015. https://doi.org/10.1016/j.jcms.2015.06.043.
38. Marcus H, Schwindack C, Santarius T, Mannion R, Kirollos R. Image-guided resection of spheno-orbital skull-base meningiomas with predominant intraosseous component. *Acta Neurochir.* 2013;155(6):981–988. https://doi.org/10.1007/s00701-013-1662-8.
39. Oya S, Sade B, Lee JH. Sphenoorbital meningioma: surgical technique and outcome. *J Neurosurg.* 2011;114(5):1241–1249. https://doi.org/10.3171/2010.10.JNS101128.
40. Chambless LB, Mawn LA, Forbes JA, Thompson RC. Porous polyethylene implant reconstruction of the orbit after resection of spheno-orbital meningiomas: a novel technique. *J Cranio-Maxillofacial Surg.* 2012. https://doi.org/10.1016/j.jcms.2011.01.016.